4.3 Preservation of Wing Leading Edge Suction at the Plane of Symmetry as a Factor in Wing-Fuselage Design

E. Eugene Larrabee
Massachusetts Institute of Technology

Abstract

Most fuselage geometries cover a portion of the wing leading edge near the plane of symmetry, and it seems reasonable to expect that a large fraction of the leading edge suction which would be developed by the covered wing at high angles of attack is not developed on the fuselage. This is one of the reasons that the Oswald span efficiency factor for the wing body combination fails to approach the value predicted by lifting line theory for the isolated wing. Some traditional and recent literature on wing-body interference is discussed and high Reynolds number data on wing-body-nacelle drag are reviewed. An exposed central leading edge geometry has been developed for a sailplane configuration. Low Reynolds number tests have not validated the design concept.

Figure 1 illustrates the significance of leading edge suction in reducing wing drag at high angles of attack. The sketch on the upper left hand side of the figure gives the airload, normal to the chord, of a symmetrical airfoil at a moderate angle of attack. The sketch on the lower left hand side compares the experimental variation of drag that would be observed in the absence of leading edge suction -- the skin friction drag plus the load normal to the chord times the angle of attack in radians. It is seen that leading edge suction -- the chordwise component of the negative pressures acting on the wing leading edge -- reduces the variation of drag coefficient with lift coefficient to a very low level for $-1 < c_\ell + 1$; in particular, for $c_\ell = +0.4$, the leading edge suction is about 5 times the skin friction drag component.

The right side of Figure 1 raises the question, for the case of a finite span wing body combination, what happens to the leading edge suction that would have been developed by the wing now covered by the fuselage, the most intense leading edge load developed anywhere on the wing.

J. Lennertz[1] attempted to answer the related matter of lift carry-over for the case of a lifting line interrupted by a cylindrical fuselage having circular cross sections and aligned with the direction of flight in 1927. He showed that the circulation at the wing root is "mirrored" on the convex fuselage sides so that the

circulation is somewhat reduced (compared to the isolated wing) in the fuselage region. The lift carry over in the fuselage region is concentrated longitudinally near the lifting line, and nearly disappears in one fuselage diameter either in the up or downstream directions. The question of the leading edge suction in the chord direction (assuming symmetrical wing airfoil sections) is unresolved because the "infinitely" long fuselage is at zero angle of attack.

The problem of calculating the lift distribution for a wing body combination is now routinely solved with high speed digital computers, using any of several finite element - discrete singularity techniques for representing the flow field around a wing body combination in such a way as to align the flow with the body surface at many control points and to satisfy the Kutta-Joukowski condition at the wing trailing edge. Such a finite element calculation has been carried out by H. Korner[2] in a form which permits direct comparison with Lennertz's analytic result. Figure 2, taken from his paper, compares the lift distribution on wing body combinations with finite wing angle of attack, and fuselage angles of attack equal to wing angle of attack, or zero (the Lennertz case) with isolated wing lift.

It is seen that the zero fuselage angle of attack case agrees with Lennertz's result (Figure 1) and that the fuselage angle of attack equal to the wing angle of attack case is very similar. Unfortunately, finite element representations of the flow field near wing body combinations do not lend themselves to drag calculation, and so we do not know whether Lennertz's analytically derived relation for the reduction of Oswald's span efficiency factor

$$e = \frac{[(b/b_f)^2 - 1]^2}{(b/b_f)^4}$$

for the case of zero fuselage angle and varying wing angle holds approximately for the fuselage angle equal to the wing angle or not.

Next we examine, in Figure 3, some model build up data in which an unusually large portion of the wing was covered by the fuselage and two nacelles. The experimental drag coefficients (containing the usual corrections for attachment drag, alignment drag, and wall restraint) are plotted versus the square of the lift coefficient to aid in fitting parabolic polars to the data.

The resulting value of e, the Oswald span efficiency factor, are plotted on Figure 4 as a function of the fraction of the wing span covered, together with Lennertz's relation. It is seen that the addition of the fuselage to the wing, or to the wing nacelle combination, causes an appreciable drop in e about twice the size

expected from Lennertz's relation. Addition of the nacelles to the wing does not cause such a large charge, apparently because the wing leading edge suction was transferred to the leading edges of the relatively short nacelles (there was no flow through the nacelles, which were provided with well rounded, cylindrical leading edges), but that the suction developed by the portion of the wing covered by the fuselage was not transferred to the fuselage nose, which is more than one local chord upstream. It is also difficult to justify the low Oswald span efficiency factor of 0.804 for the isolated wing; it may be related to side edge vortex formation due to flow around the streamwise wing tip. Figure 4 also includes a point obtained in a full scale test of the Twin Commanche airplane, showing that the loss of Oswald span efficiency factor seen with XP-87 wind tunnel model is not unusual.

Figure 5 shows an innovative geometry for a sailplane, intended to preserve leading edge suction at the plane of symmetry by the simple expedient of exposing the leading edge from 20% chord on the lower surface to 20% chord on the upper surface. Additionally the tail assembly and the pilot's pod are attached to the wing by structures of minimum aerodynamic interference. The object is to obtain an Oswald span efficiency factor approaching 1 and to minimize stalling at the wing-tail boom junction so that $C_L^{3/2}/C_D$ can be maximized in circuling flight to improve rates of climb in weak thermals[3].

Figure 6 presents the results of an abortive wind tunnel program to verify this design feature. A wing body combination was tested as a mid wing (leading edge covered) and as a pylon wing arrangement at a low Reynolds number in a quiet tunnel where laminar separation might be expected to be an important aspect of the flow. The endplating of the wing was poor at the top of the tunnel, where air loads on the wing forced open the wing tip-ceiling gap by increasing amounts with increasing lift. The pylon arrangement had more skin friction (the pylon plus the exposed wing area) and it is uncertain whether the slight trend to lower drag at the highest values of C_L^2 is valid or not. A better test is contemplated in the near future.

---

(1) Lennertz, J., "Beitrag zur Theoretischen Behandlung des gegenseitigen Einflusses von Tragflache und Rumpf" (Contribution to the Treatment of the Opposing Effects of Wing and Body Abhandlungen aus der Technische Hochshule Aachen Heft. 8, 1928.

(2) Korner, H., "Theoretische Parameter Untersuchungen an Flugel-Rumpf-Kombinationen," (Theoretical Parameter Studies on Wing Body Combinations) Deutsche Forschungs-und Versuchsanstalt fur Luft-und Raumfahrt, Institute fur Aerodynamic Braunschweig FB 72-63.

(3) Larrabee, E.E., "Lateral Control and Saiplane Design Considerations to Optimize Altitude Gain While Thermalling," AIAA Paper 74-1004.

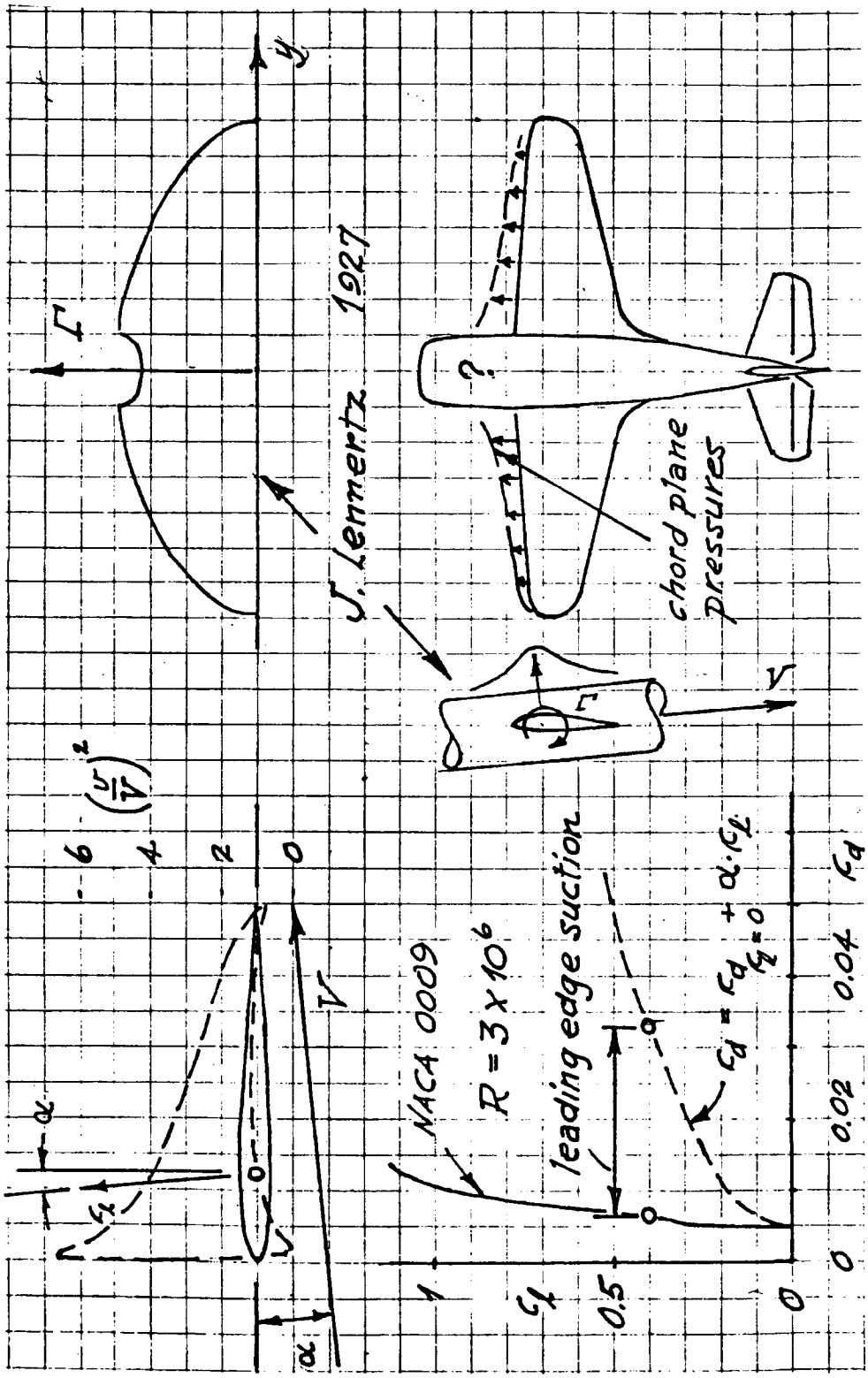

Figure 1. Drag Significance of Leading Edge Suction

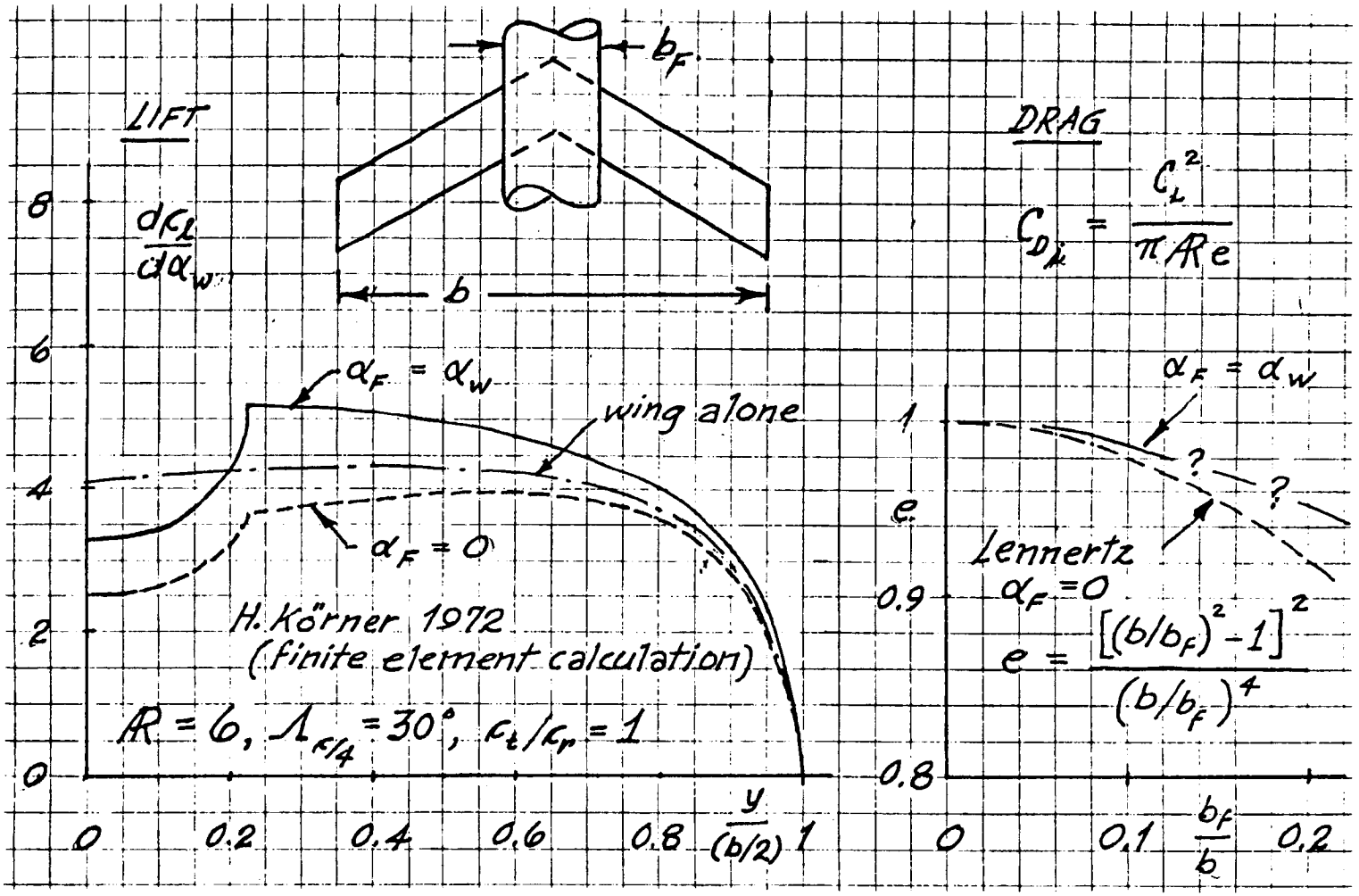

Figure 2. Fuselage Effects on Lift and Drag

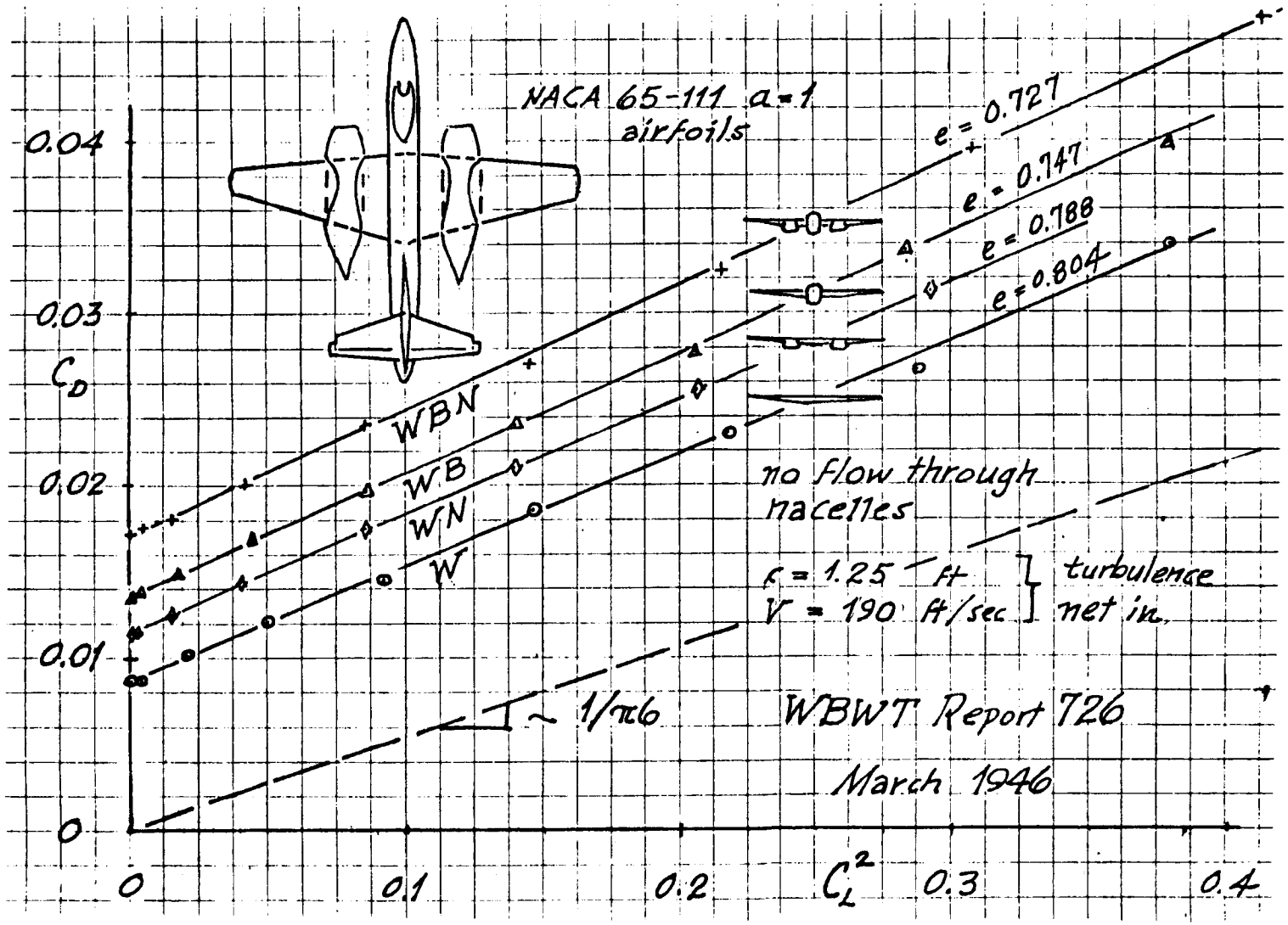

Figure 3. XP-87 Wind Tunnel Model Results

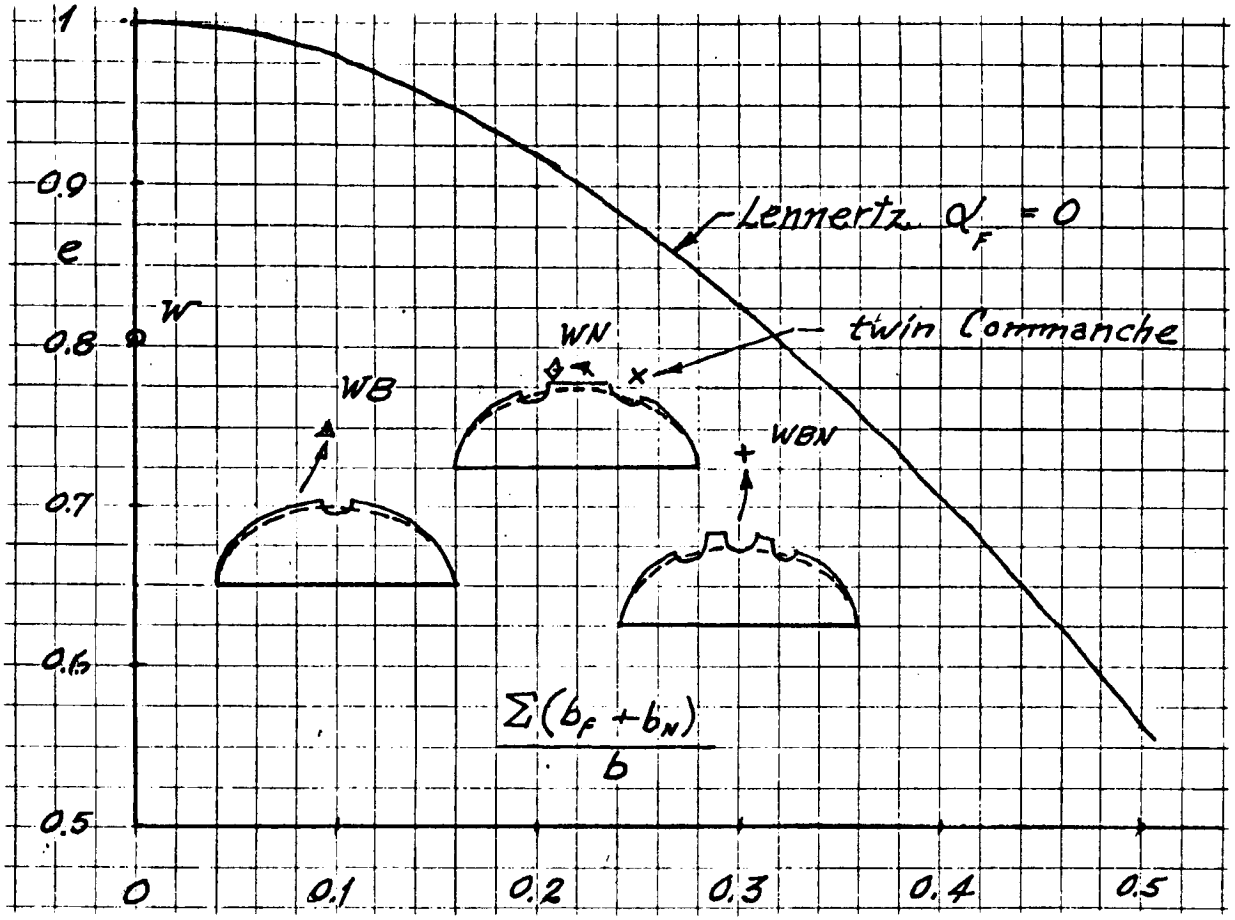

Figure 4. XP-87 Results vs. Lennertz's Theory

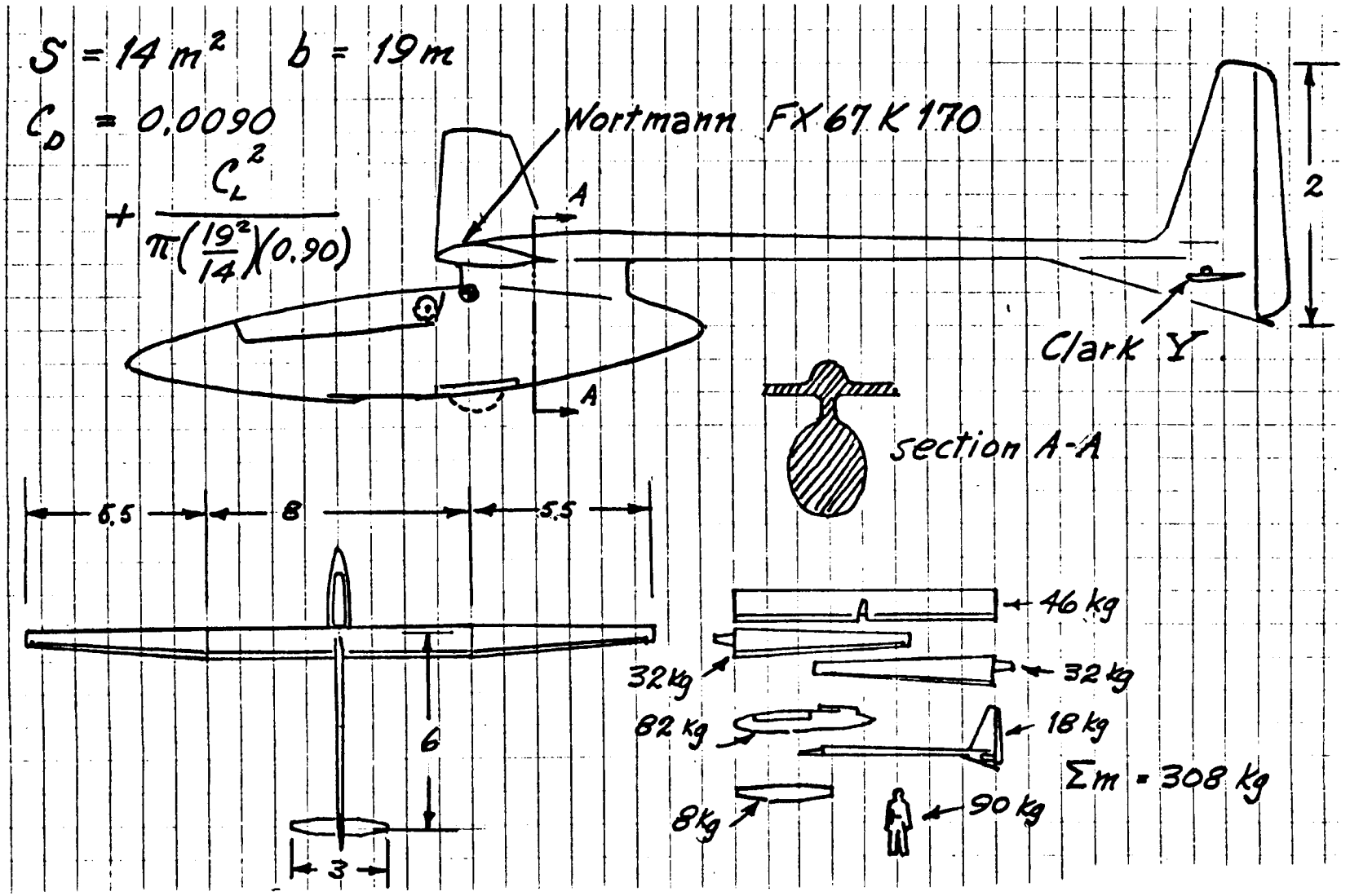

Figure 5. Example Sailplane

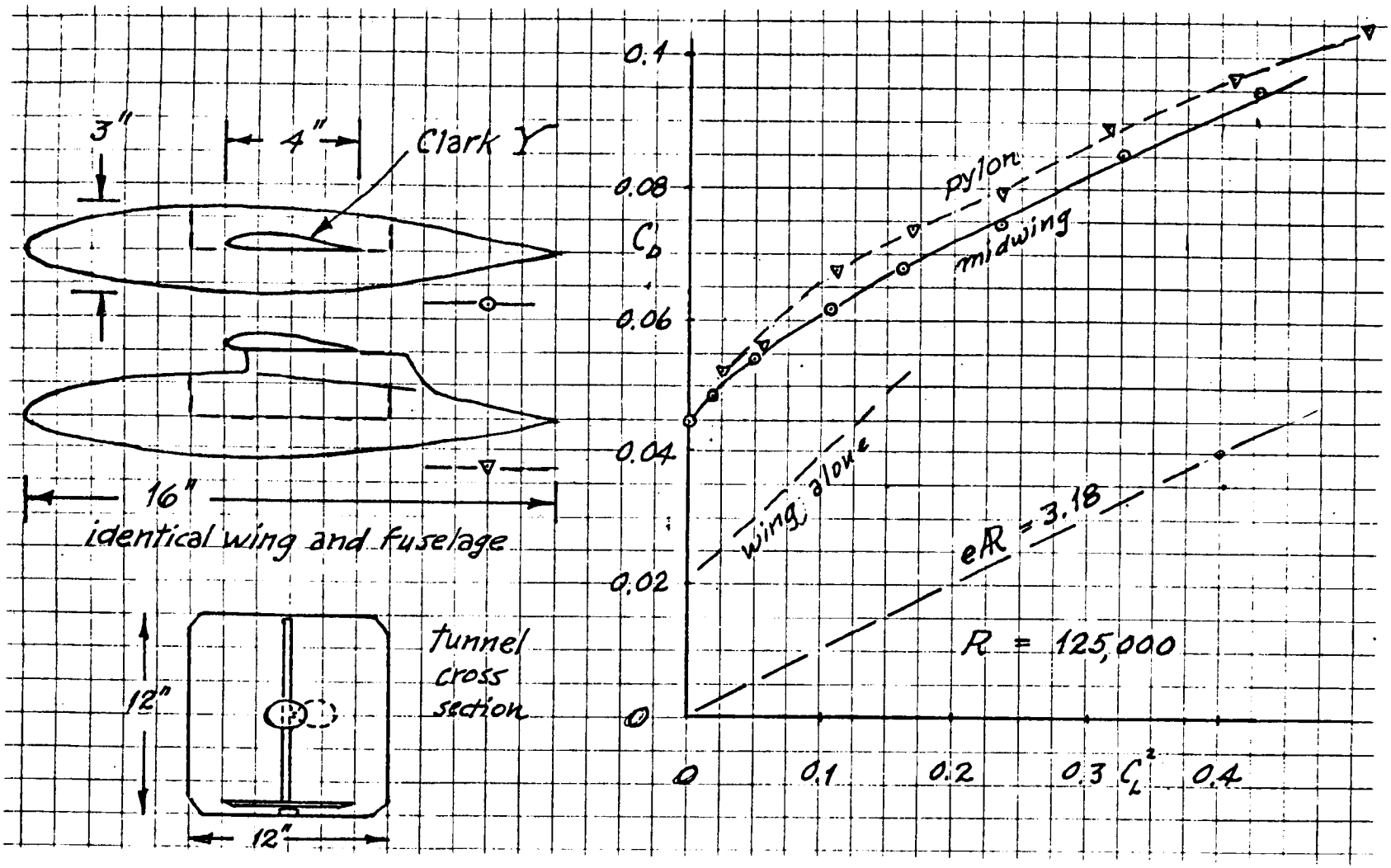

Figure 6. Exposed Central Leading Edge Experiment